

Characterization and self-assembly of poly [sodium *N*-(11-acrylamidoundecanoyl)-L-alaninate] in water

Rati Ranjan Nayak, Sumita Roy, Joykrishna Dey *

Department of Chemistry, Indian Institute of Technology, Kharagpur 721 302, India

Received 10 March 2005; received in revised form 3 September 2005; accepted 23 October 2005

Available online 14 November 2005

Abstract

A vesicle-forming amino acid derivatized surfactant, sodium *N*-(11-acrylamidoundecanoyl)-L-alaninate was polymerized to obtain a polysoap. The average molecular weight of the polysoap was determined by gel permeation chromatography. Rheological measurements suggested that the aqueous solution of the polysoap behaves as a non-Newtonian fluid. Fluorescence probe studies using pyrene as probe molecule indicated hydrophobic domain(s) (intra-chain aggregate) formation within a polymer chain. It has been found that the vesicular structure formed by surfactant monomers are retained after polymerization. The polymer forms inter-chain aggregates in concentrated solution. The dependence of fluorescence anisotropy of 1,6-diphenyl-1,3,5-hexatriene on temperature, pH, and urea concentration suggested strong inter-chain interactions of the polysoap. The pK_a of the surfactant units of the polymer chain and the phase transition temperature were determined. Dynamic light scattering measurements were performed to determine the mean size of the aggregates. The size of the aggregates was found to increase with the increase in polymer concentration also suggesting formation of inter-chain aggregates. The transmission electron micrographs revealed closed vesicular structures in water.

© 2006 Elsevier Ltd. All rights reserved.

Keywords: Polysoap; Vesicles; Fluorescence

1. Introduction

Amphiphilic molecules in aqueous solution self-assemble to form a variety of microstructures, for example micelles, vesicles, tubules, and rods, etc. above a certain concentration and have been a subject of intensive research during the past 4 decades [1–3]. The microstructures formed by the amphiphiles are in dynamic equilibrium with the surfactant monomer in solution. The equilibrium morphology of the self-assembled system depends on the geometric factors such as the ratio of the sizes of ‘head group’ and hydrocarbon ‘tail’ of the amphiphile. For example, vesicular structures are usually formed by double-tailed amphiphiles [4]. However, in recent literature, single-tailed amphiphiles have also been reported to form bilayer vesicles [5–7]. The vesicles have two distinct domains: the lipophilic membrane and the interior aqueous cavity. They can entrap large quantities of reagents either in the lipophilic membrane or in the aqueous cavity. Therefore, vesicles formed

by synthetic surfactants have attracted tremendous attention because of their potential uses as agents for encapsulation and eventual release of drugs, flavors, and fragrances, and also as microreactors for the synthesis of monodispersed nano-sized semiconductor particles [8]. Recently, vesicles have been also proved to be very useful in chromatographic separations of various molecules including biomolecules [9]. Normally, the vesicles are formed by disruption of bilayer phases by sonication. However, these metastable vesicles ultimately transform into the more stable bilayer lamellar structures from which they were formed. This limits their use in applications mentioned above [10]. Therefore, generation of stable vesicles in aqueous solutions of synthetic surfactants have received much attention. One way to obtain structural stabilization of vesicles is chemically tethering of the surfactant monomers through polymerization. To be able to do so surfactant monomers that incorporate a polymerizable group such as vinyl moiety are required. The short chain surfactant monomers can then be incorporated into the polymer backbone through polymerization of the vinyl group. The resulting polymeric soaps are capable of forming both intra-chain and inter-chain aggregates of a variety of morphologies. The polymeric soaps with number average molecular weight of about 2000 Da are referred to as ‘polymeric micelles’ and those

* Corresponding author. Tel.: +91 3222 283308; fax: +91 3222 255303.

E-mail address: joydey@chem.iitkgp.ernet.in (J. Dey).

with high molecular weight (10^5 – 10^6 Da) are called as ‘polysoaps’ [11]. Recognizing the need for stable vesicles, many authors have synthesized both cationic as well as anionic polymerized surfactant vesicles [12–14]. The vesicles formed by polysoaps are reported to be more stable than those formed by monomeric ones, and therefore, expected to act as better encapsulants of cosmetic substances and pharmaceutical drugs. One of the interesting properties of polysoaps is that they exhibit secondary structure due to the intra-chain micellization. Therefore, polysoaps can be viewed as a primitive model system for proteins. Both systems undergo configurational changes upon addition of free surfactants.

It has been shown that single-chain *N*-acylamino acid surfactants (NAAS) spontaneously form vesicles, tubules and helical ribbons suggesting ordered bilayer membranes in dilute aqueous solution [7,15–17]. Recently, we also have shown that sodium salt of *N*-(11-acrylamidoundecanoyl)-L-alanine (SAUA) spontaneously forms bilayer aggregates including vesicles and helical ribbons in aqueous solutions [18]. The NAAS have attracted considerable attention mainly because of their chirality, which is an important phenomenon in nature [16]. The sodium salts of long-chain NAAS have wide applications in detergents, foaming agents, and shampoos, as they are mild, non-irritating to human skin, and easily biodegradable [17]. One of the most important properties of these supramolecular assemblies formed by NAAS is chiral recognition. The chiral recognition properties of the monolayers of NAAS have recently been reported [16]. On the other hand, chiral discrimination by these surfactants in solution has been exploited by separation scientists [19]. Several monomeric as well as polymerized NAAS have been synthesized and used as stationary and pseudo-stationary phases in liquid chromatography for enantiomeric separation of pharmaceutical drugs, pesticides, and insecticides [20]. It has been found that in most of the cases, the chiral polymeric micelles act as better chiral selectors than their monomeric counterparts. However, no appropriate explanation has been offered for this observation. We believe that this behavior must be related to the morphological changes of the aggregates that are formed in solution. In order to shed light on this, we have synthesized a novel polysoap, poly[sodium *N*-(11-acrylamidoundecanoyl)-L-alaninate], PSAUA (see inset of Fig. 1 for structure) to (i) characterize it in aqueous solution, (ii) investigate its self-organization in water, (iii) study the microenvironment of the self assemblies, (iv) determine the mean size of the self assemblies and (v) investigate the microstructure of the self assemblies in aqueous solution.

2. Experimental section

2.1. Materials

The fluorescence probes pyrene, and 1,6-diphenyl-1,3,5-hexatriene (DPH) (Aldrich) were recrystallized from acetone–ethanol mixture at least three times. Purity of these probes was tested by the fluorescence emission and excitation spectra. Acryloyl chloride (Aldrich) and 11-aminoundecanoic acid

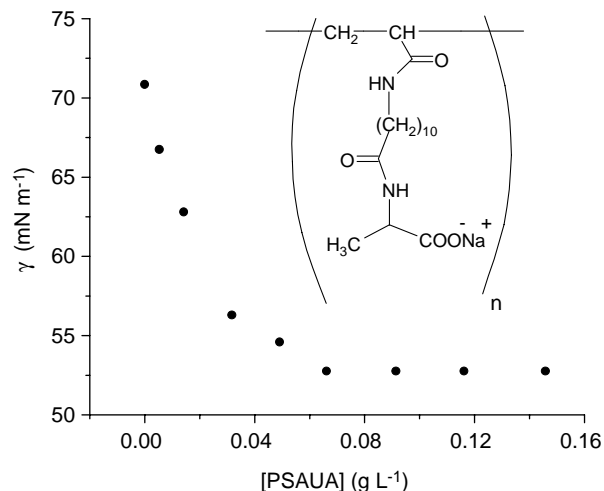


Fig. 1. Surface tension (γ) versus [PSAUA] plot; inset: chemical structure of poly[sodium *N*-(11-acrylamidoundecanoyl)-L-alaninate].

(Aldrich), *N*-hydroxysuccinimide (SRL), dicyclo-hexylcarbodiimide, (SRL) and L-alanine (SRL), were used without further purification. Potassium persulfate $K_2S_2O_8$ (MERCK) was recrystallized from water. Analytical grade sodium acetate, sodium dihydrogen phosphate, disodium hydrogen phosphate, sodium hydroxide, sodium bicarbonate, hydrochloric acid were procured locally and were used directly from the bottle. All solvents used were of good quality commercially available and whenever necessary purified, dried, and distilled fresh before use.

2.1.1. Synthesis of polysoap

The *N*-(11-acrylamidoundecanoyl)-L-alanine (AUA) was synthesized from *N*-hydroxysuccinimide ester of 11-acrylamidoundecanoic acid (AU) and L-alanine by slight modification of the method reported in the literature [21]. The AU was synthesized and purified according to the procedure described elsewhere [22]. SAUA (2 gm, 60 mM) was dissolved in 100 mL of water in a three-neck polymerizing vessel equipped with condenser and gas inlet–outlet tube. The solution was degassed for about an hour to remove dissolved oxygen and the polymerization was then initiated by the addition of 15 mg (0.6 mM) of solid $K_2S_2O_8$ through a small port. Mixture was stirred for 2 h under a positive pressure of N_2 at 60 °C. The resulting viscous solution indicated formation of polymer. The polymer solution was dialyzed for 72 h using 12 kDa molecular weight cut off dialysis bag against alkaline water (pH = 9) with frequent change of water and then lyophilized to get poly[sodium *N*-(11-acrylamidoundecanoyl)-L-alaninate] (PSAUA). The polymerization was confirmed by the disappearance of the vinyl proton peaks between δ values 5.0 and 7.0 in the 1H NMR spectrum of PSAUA in D_2O . Also the broadness of the peaks suggested polymeric structure of PSAUA. Further, the FT-IR spectrum of the polymer showed no olefinic C–H, C=C stretching frequency around 3050 and 1624 cm^{-1} , respectively, confirming the polymeric structure. The specific rotation $[\alpha]_D^{25}$ (H_2O , c 0.20) = -14° confirmed optical activity of the polymer.

2.2. Methods

2.2.1. General instrumentation

¹H NMR spectra were recorded on a Bruker SEM 200 instrument in CDCl₃ or D₂O solvents using TMS as standard. The FT-IR spectrum was measured with a Thermo Nicolet Nexus 870 spectrometer. The UV-visible spectra were recorded in a Shimadzu (model 1601) spectrophotometer. The optical rotation of PSAUA was measured with a Jasco P-1020 digital polarimeter. The differential scanning calorimetric measurements were performed with a Perkin Elmer model Pyris Diamond DSC instrument. Melting points were determined with Instind (Kolkata) melting point apparatus in open capillaries. The pH measurements were done with Thermo Orion model 710A+ digital pH meter.

2.2.2. Gel permeation chromatography

For molecular weight determination by GPC the protonated form of the polysoap, PSAUA was employed. GPC was performed at 40 °C with a setup consisting of a Waters 515 HPLC pump and High MW column: Polymer Labs-Plgel 5 μm. Mixed C (300×7.5 mm²). The isocratic flow rate was set at 1.0 mL/min using uninhibited DMF as the mobile phase and the elution of the sample was monitored with RI (refractive index) detector. The elution times were converted to molecular weights with a calibration curve constructed from narrow polydispersity polymethylmethacrylate (PMMA) standards (High MW standards: Polymer Labs-(M-M-10 Kit:1000–1.5 m range)). A dilute polymer solution (0.037%) prepared in DMF was injected into the 20 μL sample loop. The calculation of molecular weight and polydispersity index were done by Waters Millennium software (version 4.0).

2.2.3. Surface tension

The surface tension measurements were performed with a Torsion Balance (Hardson & Co., Kolkata, India) using Du Nuoy ring detachment method. The platinum–iridium ring was carefully cleaned with 50% ethanol–HCl solution and finally with distilled water. The ring was carefully flamed before measurement. The glassware was thoroughly cleaned with sulfochromic acid and water. The instrument was calibrated and checked by measuring the surface tension of distilled water. A stock solution of PSAUA was made in Milli-Q water (18.2 MΩ). Aliquot of this solution was transferred to a beaker containing known volume water. The solution was gently stirred magnetically and allowed to stand for about 5 min at room temperature (~30 °C) and then surface tension was measured. For each measurement at least three readings were taken and the mean γ value was recorded.

2.2.4. Light scattering

The dynamic light scattering (DLS) measurements were performed with a Photal DLS-7000 (Otsuka Electronics CO. Ltd., Osaka, Japan) optical system equipped with an Ar⁺ ion laser (75 mW) operated at 16 mW at λ₀=488 nm, a digital correlator, and a computer-controlled and stepping-motor-driven variable angle detection system. The solutions were

filtered through a micro syringe filter (0.22 μm) to the scattering cell. Before measurement, the scattering cell was rinsed several times with the filtered solution. The DLS measurements started 5–10 min after the sample solutions were placed in the DLS optical system to allow the sample to equilibrate at the bath temperature. The data acquisition was carried out for 10 min and each experiment was repeated two or three times. The data were analyzed using cumulant method. For all light scattering measurements, the temperature was 25 ± 0.5 °C.

2.2.5. Rheology

A stress-control type rheometer (AR.1000 Rheometer, TA instruments, USA) was used to measure the flow properties of the polymer solutions. A parallel plate with a diameter of 4 cm was employed. In the flow properties measurements, the flow curves were obtained after the sample was kept under stress for 1 min, which then reduced to zero within 1 min. All measurements were done at room temperature (~30 °C) after 24 h of sample preparation.

2.2.6. Steady-state fluorescence spectra

The steady-state fluorescence spectra were measured on a SPEX Fluorolog-3 spectrofluorometer. Stock solutions of pyrene was prepared by adding the compound to Milli-Q (18.2 MΩ cm⁻¹) water and magnetically stirred at 40 °C for 24 h. After equilibrating at room temperature the excess compound was removed by filtration through Millipore syringe filter (0.22 μm). A weighed amount (2 g L⁻¹) of the polymer was added to the saturated probe solution. This was used as polymer stock solution. Appropriate volume of probe stock solution was used to make various dilutions of the polymer stock solution. The pyrene solutions were excited at 335 nm and the emission was recorded in the wavelength range 350–500 nm. The excitation and emission slit with band-pass equal to 1 nm was used for fluorescence measurements. All fluorescence measurements started after 24 h of sample preparation.

2.2.7. Fluorescence depolarization measurements

Steady-state fluorescence anisotropy (*r*) of DPH was measured on a Perkin Elmer LS-55 luminescence spectrometer equipped with filter polarizers that uses the L-format configuration. The temperature of the water-jacketed cell holder was controlled by use of a Thermo Neslab RTE 7 circulating bath. Since DPH is insoluble in water, a 1 mM stock solution of the probe in 20% (v/v) methanol–water mixture was prepared. The final concentration of the probe was adjusted to 5 μM by addition of an appropriate amount of the stock solution. The sample was excited at 350 nm and the emission intensity was followed at 450 nm using excitation and emission slits with band-pass of 2.5 and 5 nm, respectively. The *r*-value was calculated employing equation:

$$r = \frac{I_{VV} - GI_{VH}}{I_{VV} + 2GI_{VH}} \quad (1)$$

where I_{VV} and I_{VH} are the fluorescence intensities polarized parallel and perpendicular to the excitation light, and G is the instrumental correction factor ($G=I_{VV}/I_{VH}$).

2.2.8. Transmission electron microscopy (TEM)

For TEM measurements, the polymer solution was filtered by use of a one-way syringe membrane filter (0.22 μm). A drop of the aqueous polymer solution (0.02 or 0.25 g L^{-1}) was placed on the 400 mesh carbon-coated copper grid, blotted with filter paper, and negatively stained with a freshly prepared 2% aqueous solution of phosphotungstic acid the pH of which was adjusted to sample solution pH (7.5) by adding 1 M KOH. The specimens were examined on a Hitachi H-600 electron microscope operating at 50 kV at room temperature.

3. Results and discussion

3.1. Molecular weight of PSAUA

The weight average molecular weight (M_w) of the polysoap was obtained by GPC. The chromatogram (not shown) exhibited two peaks, a major peak (80%) with narrow molecular weight distribution (polydispersity index, $\text{PDI}=1.06$) resulted a M_w value of 6.42×10^6 and a second peak (20%), which is relatively broad ($\text{PDI}=1.26$) gave M_w equal to 2.88×10^5 . The weight average molecular weights thus obtained are very high. Similar value of M_w has also been reported by others for structurally similar polysoap poly(sodium 11-acrylamidoundecanoate), PSAU [23]. Since the surfactant monomer forms bilayer vesicles in water [18], polymerization can either take place among surfactant monomers in the same layer (i.e. linear polymerization) or by zipping-up of the monomers of both layers of the bilayer assembly. In the later case, the molecular weight is expected to be higher. The large M_w value suggests that perhaps the latter mechanism may be true with the SAUA vesicles. Since the vesicles of SAUA have been reported to have broad size distribution [18], the low molecular weight polymers might have formed from smaller vesicles. However, the PDI values as obtained from GPC are very low. That is PSAUA has a narrow molecular weight distribution as expected. This is because the polymerization was carried out in aqueous solution in a state of aggregation.

3.2. Surface activity of PSAUA

In order to examine the surface activity of the polysoap, surface tensions were measured in water at different concentrations of the polysoaps. The plot of surface tension (γ) versus concentration of the polysoap is shown in Fig. 1. The plot shows a moderate decrease of surface tension of water suggesting that the surface activity of the polysoap is as good as the monomer [18]. The breakpoint ($\sim 0.1 \text{ g L}^{-1}$) in the plot may be taken as critical aggregation concentration (cac) of the polymer for reasons described below.

3.3. Flow behavior of PSAUA

From its application point of view the study of rheological properties of synthetic polymers is very important. The rheological properties of aggregating polymer solutions are reported to be strongly dependent on their morphologies and phase behavior. To examine whether the PSAUA really forms any aggregate we have investigated the flow behavior of its aqueous solutions at different concentrations. Fig. 2 shows the representative flow curves of aqueous solutions of PSAUA at two concentrations at room temperature. The plots indicate a non-Newtonian flow behavior of the polymer. The feature of the plots clearly indicates that the flow behavior of the polymer solution is shear thinning with yield stress, which means decrease of apparent viscosity with increasing shear rate. The flow behavior (inset Fig. 2) of the solutions containing 0.5 and 2.0 g L^{-1} PSAUA suggests that there exists some heterogeneous structure, such as micelles [24]. This substantiates the observation of aggregation of the polysoap and is consistent with the results obtained from surface tension studies.

3.4. Hydrophobic domain formation

If there is any formation of hydrophobic domain in the polymer chain, then it should be reflected by the micropolarity of the domain. Pyrene is a well-known fluorescence probe for the micropolarity studies of its solubilization site in micellar interior [25]. The intensity ratio I_1/I_3 of the first and the third vibronic peaks of the pyrene fluorescence spectrum has been widely used as a measure of the polarity of the microenvironment of the probe [26,27]. Normally, high I_1/I_3 ratio indicates polar environment and low I_1/I_3 value suggests less polar or non-polar environment. The I_1/I_3 ratio was determined in the concentration range 0–1.0 g L^{-1} at pH 8.0. The plot in Fig. 3 shows that the polarity ratio decreased to a value equal to 1.38, which is much less than that in water (1.84). The concentration corresponding to the inflection point can be taken as the cac

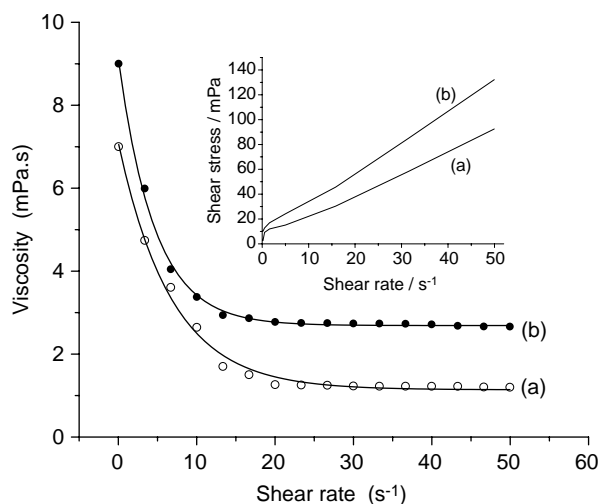


Fig. 2. Plot of viscosity versus shear rate for (a) 0.5 g L^{-1} , and (b) 2 g L^{-1} PSAUA; inset: flow behavior of (a) 0.5 g L^{-1} , and (b) 2 g L^{-1} PSAUA in water.

value (0.137 g L^{-1}). The cac value thus obtained is closely similar to that obtained from surface tension measurements. The absence of any concentration-independent region below cac suggests that hydrophobic domains are also present within a polymer chain. The low I_1/I_3 value above cac indicates that the probe is solubilized in a less polar environment of the inter-chain aggregate compared to that in intra-chain aggregate. The low polarity of the local environment of the probe in inter-chain aggregate suggests that the fluorophore is solubilized in the interior of the aggregate and the aggregate surface is highly ordered. The ordering of the aggregate interface is a result of reduced degree of water penetration in the hydrocarbon layer, in accordance with the reduction observed in micropolarity sensed by the probe molecules. It should be noted that the polarity ratio in 0.25 g L^{-1} PSAUA solution is less than that in the bilayer self-assemblies formed by monomeric SAUA (1.42) [18]. This means that the pyrene probe experiences more hydrophobic environment in inter-chain aggregates as compared to unpolymerized vesicles.

In order to investigate the ordering of the hydrocarbon chains in the aggregate interior, we have measured steady-state fluorescence anisotropy (r) of DPH probe in the presence of PSAUA. DPH is a well-known membrane fluidity probe and has been used for studying many lipid bilayer membranes [28, 29]. The fluorescence spectrum of DPH shows enhancement of intensity (not shown here) accompanied by a small blue shift in the presence of polymer relative to that in water indicating solubilization of the probe molecule in non-polar environments. The plot of concentration dependence of r is shown as inset of Fig. 3. The r -value can be found to increase with polymer concentration and labels off above 0.25 g L^{-1} PSAUA solution at pH 8. The breakpoint of the plot suggests formation of inter-chain aggregates above the cac as already established by rheology and surface tension studies, and also by fluorescence titration using pyrene as probe molecule. The cac value (0.12 g L^{-1}) obtained from the breakpoint is exactly equal to that obtained from pyrene fluorescence measurements. The relatively high value of r suggests an ordered environment around the DPH probe in the assemblies. That is the

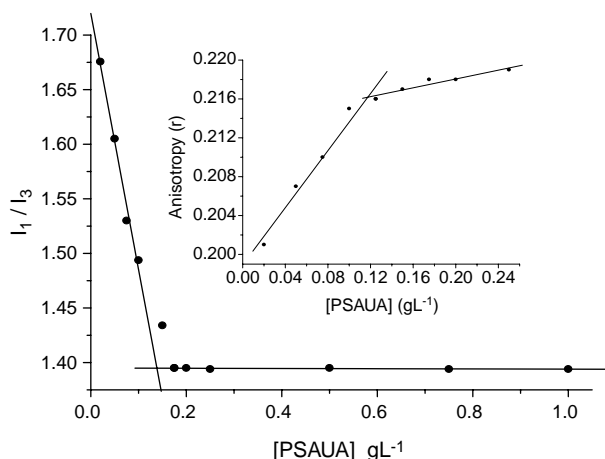


Fig. 3. Plot of I_1/I_3 ratio against polymer concentration at pH 8.0; inset: plot of fluorescence anisotropy of DPH versus polymer concentration at pH 8.0.

hydrocarbon chains of the surfactant units are tightly packed in the inter-chain aggregates. This might be due to the amide hydrogen bonding between two adjacent surfactant units in the polymer chain. The high anisotropy value perhaps indicates the presence of three-dimensional lamellar structure formed through inter-chain association. It should be noted that the anisotropy value in PSAUA at pH 8.0 (0.220) is large compared to that in SAUA (0.180) [18] at the same pH. This is consistent with the results suggested by the respective polarity ratio. This indicates that the probe experiences a more rigid environment in the polymerized vesicles compared to unpolymerized vesicles. That is in the case of inter-chain aggregates the hydrocarbon chains are more tightly packed than in unpolymerized vesicles. This might be due to the rigidity of the polymer chain. The stability of the intra- and inter-chain aggregates is further confirmed by the temperature dependence of fluorescence anisotropy in dilute and concentrated polymer solutions as discussed below.

3.5. Dynamic light scattering (DLS) studies

The DLS experiments were aimed at elucidating the structure of the polymer at various concentrations. The DLS measurements provide evidence of the structural evolution of the system as the concentration is increased. Therefore, we have measured the translational diffusion coefficient (D) of the polymer at two concentrations, one below cac and the other at above cac by use of DLS technique. The scattering intensity was measured in the angular range of $20^\circ < \theta < 120^\circ$ corresponding to $4.47 \times 10^{-3} \text{ nm}^{-1} < q < 2.23 \times 10^{-2} \text{ nm}^{-1}$ to check the angular dependence of the decay rate (Γ). The slope of the plot (Fig. 4) of decay rates versus square of the scattering vector (q^2) gave the apparent translational diffusion coefficient. From the diffusion coefficient, hydrodynamic radius (R_h) of the polymer was calculated using Stokes–Einstein equation. It has been found that the R_h value increases in going from dilute (17 nm) to concentrated (60 nm) solution.

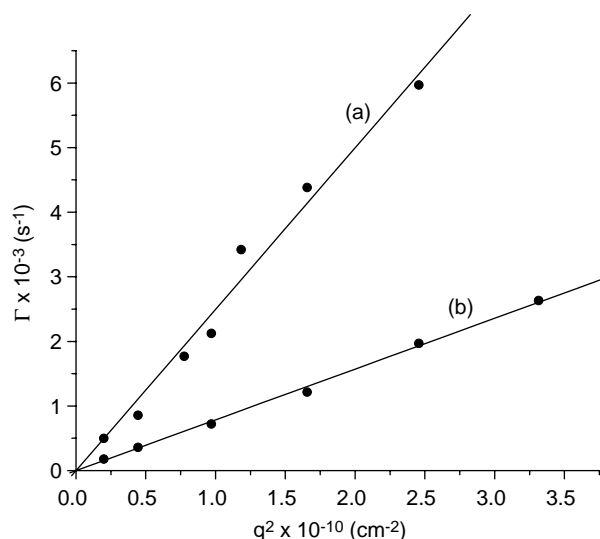


Fig. 4. Plot of Γ versus q^2 (a) 0.02 g L^{-1} (b) 0.25 g L^{-1} .

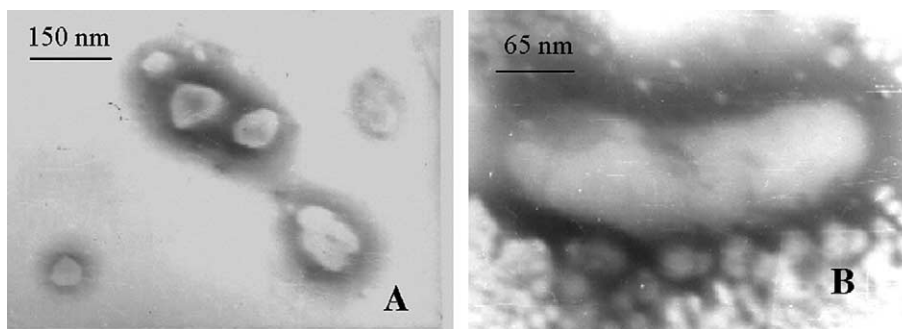


Fig. 5. Negatively stained transmission electron micrographs of (A) 0.02 g L^{-1} (B) 0.25 g L^{-1} PSAUA in water at $30 \text{ }^\circ\text{C}$.

3.6. Transmission electron microscopy

The TEM studies were carried out to investigate the morphologies of the intra- and inter-chain aggregates of the polysoap in water. Fig. 5 shows the TEM images of the aqueous solutions of PSAUA. It can be found that polydispersed and slightly distorted spherical shaped vesicles (Fig. 5(A)), are formed at low concentrations. The internal diameter of the vesicles ranges between 30 and 85 nm, which are close to the sizes obtained from DLS measurements. The micrograph (Fig. 5(B)) for higher concentration also shows large spherical as well as elongated vesicles of length about 250 nm and width of 62 nm. The bilayer vesicles of similar sizes were also observed in aqueous solution of the surfactant monomer, SAUA [18]. However, at concentration higher than 0.25 g L^{-1} only lumpy masses were observed (not shown) suggesting the presence of globular type inter-chain aggregates in solution. The results of the above studies suggest that vesicular polymerization of the surfactant monomers produces polymer chains of various chain lengths. The long polymer chains themselves through intra-chain association can form small unilamellar vesicles. On the other hand the small chains by association with other polymer chains form either

unilamellar or multilamellar vesicles. The schematic presentation of formation of polymeric vesicles is shown in Fig. 6.

3.7. pH Dependence of aggregation

Since the polysoap is a polycarboxylate salt, its aggregation is expected to be pH dependent. In order to study the pH dependence we have measured pyrene fluorescence in the presence of PSAUA at different pH in the range 4.0–8.0. The plots of pH dependence of the I_1/I_3 value for two concentrations (above and below cac) of PSAUA are shown in Fig. 7. It can be observed that in both cases, the I_1/I_3 ratio increases with the increase in pH reaching the limiting value at pH 8.0. That is the pyrene probe in aqueous solutions of PSAUA experiences a more polar environment at higher pH compared to that at low pH. However, in the case of concentrated solution, the effect is less as compared to the dilute solution. Similar changes were also observed with the surfactant monomer [18]. This can be attributed to the protonation of the $-\text{COO}^-$ group, which results in a decrease in electrostatic repulsion among head groups of the surfactant units attached to the polymer chain and hence compact packing of the hydrophobic chains. Consequently, water penetration into the aggregate core is reduced which means reduction in polarity of the solubilization site of the pyrene probe. Thus the pH (6.3) corresponding to the inflection point in the plot can be taken as the pK_a of the carboxylic group. Similar value of pK_a was also obtained for SAUA monomer. In concentrated polymer solution, the relatively small change of I_1/I_3 ratio with the increase of pH may suggest only a small structural perturbation of the large inter-chain aggregates. Also the pK_a value (5.5) obtained from the plot is less than that obtained for dilute polymer solution. This may be due to the higher negative charge density of the membrane surface in concentrated solution.

The pH-induced tightening of hydrocarbon chain packing is further confirmed by the increase of fluorescence anisotropy of DPH with the decrease of pH of the solution. The plots in the inset of Fig. 7 show the variation of r as a function of pH. The increase of r -value with the decrease in pH can be observed for both dilute and concentrated solutions. However, the magnitude of change in r is less in concentrated solution in consistency with the small change in I_1/I_3 ratio. The transition pH (5.85) however, is slightly less than that obtained by use of

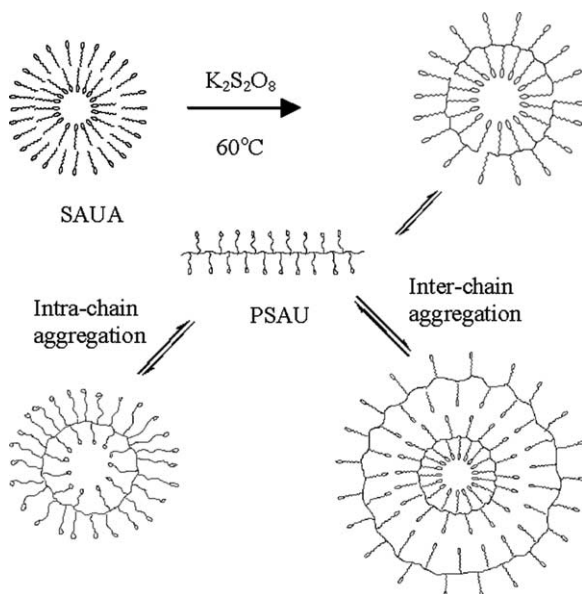


Fig. 6. Schematic representation of the formation of polymeric vesicles.

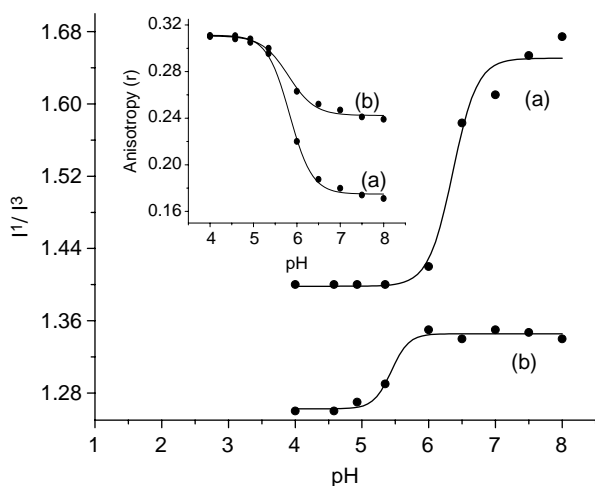


Fig. 7. Plot of I_1/I_3 ratio as a function of pH in the presence of (a) 0.02 g L^{-1} , and (b) 0.25 g L^{-1} PSAUA; inset: plot of anisotropy versus pH (a) 0.02 g L^{-1} , and (b) 0.25 g L^{-1} PSAUA.

pyrene as probe molecule. This difference can be attributed to the inherent sensitivity of the probes. Similar transition was also observed for the surfactant monomer, SAUA [18]. Therefore, as discussed in the previous paragraph this can be associated to the protonation of the carboxylate group. The partial protonation of the carboxylic acid group also results in promotion of intermolecular hydrogen bonding between $-\text{COOH}$ and $-\text{CONH}-$ groups of adjacent surfactant units further increasing the order at the interface.

3.8. Phase transitions of the polymeric membranes

Phospholipid vesicles when heated or cooled undergo distinct structural changes at a certain temperature called phase transition temperature. The phase transition temperature of PSAUA vesicles was also determined by following changes in fluorescence anisotropy of DPH probe. The variation of r as a function of temperature is shown in Fig. 8. In the case of concentrated solution, the anisotropy changes very little with

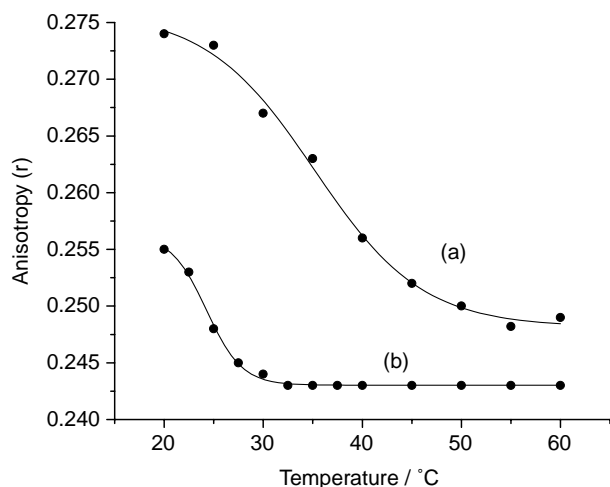


Fig. 8. Plot of fluorescence anisotropy of DPH as a function of temperature in the presence of (a) 0.01 g L^{-1} , and (b) 0.25 g L^{-1} PSAUA.

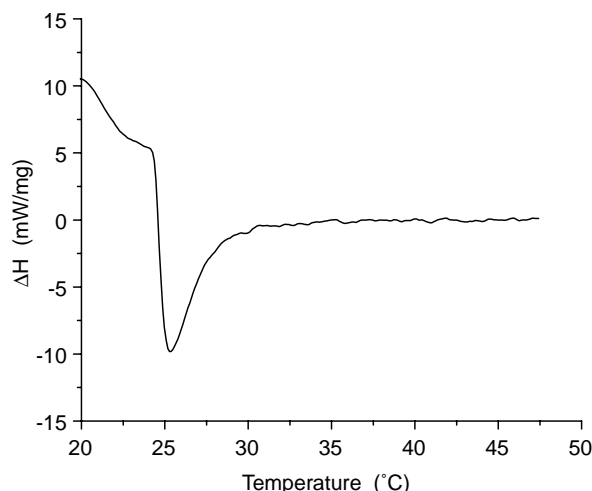


Fig. 9. DSC thermogram of 0.25 g L^{-1} PSAUA in aqueous solution; scanning rate: $0.5 \text{ }^\circ\text{C min}^{-1}$.

temperature. The inflection point ($24.3 \text{ }^\circ\text{C}$) of the sigmoid curve gives the phase transition temperature T_m , which involves change in hydrocarbon chain mobility. Similar transition temperature ($25 \text{ }^\circ\text{C}$) was also found in the thermogram (Fig. 9) obtained by differential scanning calorimetry. However, in the case of dilute solution, the magnitude of the change in r -value is large in comparison to the concentrated solution. The corresponding phase transition temperature is $35.2 \text{ }^\circ\text{C}$. This indicates relative stability of the polymeric membrane structures produced by inter-chain and intra-chain aggregation. Below the phase transition temperature the lipid chains in the bilayer are highly ordered gel states. Above the phase transition temperature lipid chains become fluid as a consequence of gauche rotations and kink formation. The observation of distinct phase transition temperature for the polysoap confirms the similarity between liposomes and completely synthetic surfactant vesicles. The relatively high transition temperature and large change in r -value relative to that of concentrated solution suggests that the intra-chain vesicles are more stable compared to the inter-polymer aggregates. This as discussed above is due to the strong intermolecular amide hydrogen bonding between pendant surfactant units in the intra-chain bilayer aggregates.

3.9. Effect of urea concentration on the vesicle structures

In order to determine stability of the polymeric vesicles and to examine the nature of interactions involved in the formation of polymeric vesicles we have investigated the influence of urea concentration on the fluorescence anisotropy value of DPH probe. Urea has been used in the past for denaturation of protein structure, which has been attributed to water structure breaking properties of urea molecules. Similar effect could be expected for the polysoap also. The dependence of anisotropy on urea concentration is plotted in Fig. 10. For dilute solution (0.01 g L^{-1}) there is a large change in anisotropy value that approaches the value obtained in the absence of polymer. This means that urea molecules destroy

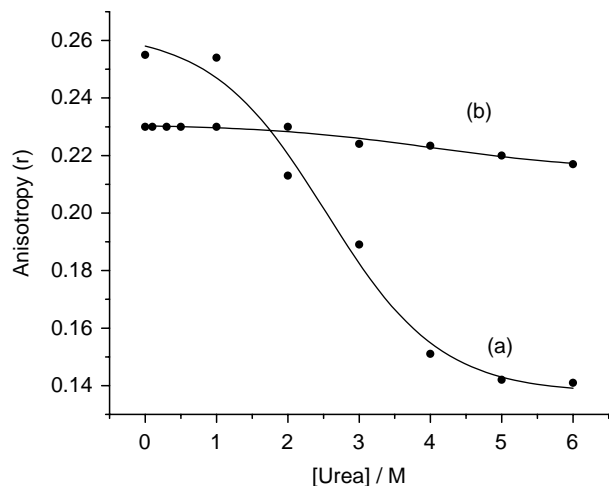


Fig. 10. Plot of fluorescence anisotropy of DPH as a function of urea concentration in the presence of (a) 0.01 g L⁻¹, and (b) 0.25 g L⁻¹ PSAUA in water.

the linear array of surfactant units attached to the polymer chain. This means that the surfactant units can dangle more freely in the presence of urea molecules. However, the surfactant units can assemble themselves to form micellar structures within the polymer chain. The sigmoid change of anisotropy value clearly indicates a two-state transition from bilayer vesicles to denatured polymer chain. At higher polymer concentration (0.25 g L⁻¹), however, the change in anisotropy is very small, which may be due to partial denaturation of the large three-dimensional lamellar aggregates. It also suggests that inter-chain interaction of the polysoap in the aggregate is very strong and non-hydrophobic in nature.

4. Conclusions

The aqueous solution of SAUA upon polymerization at concentrations above critical vesicle concentration of the surfactant produces polysoap, PSAUA with a narrow molecular weight distribution. The polysoap is equally surface active as its monomer. The polymer exhibits a non-Newtonian flow behavior in water. In dilute solutions (pH=8.0) the polymer remains as an intra-chain compact monolayer vesicle. Above critical aggregation concentration, however, PSAUA forms large multilayer vesicular structures. Each inter-chain aggregate is formed by entanglement of small polymer chains under the influence of some non-hydrophobic interactions. Both intra-chain and inter-chain vesicles are stable to change in pH, temperature, and addition of urea. The surfactant units in the polymer chain have higher pK_a value compared to free surfactant monomers in water.

Acknowledgements

The work presented in this paper was supported by CSIR, New Delhi (Grant No. 01(1664)/00/EMR-II). SR thanks CSIR for a research fellowship. RRN is thankful to IIT, Kharagpur for a research associateship. The authors are

grateful to Dr T. Goswami, Agriculture and Food Engineering Department, IIT, Kharagpur and Dr Bishwa Ranjan nayak, The University of Southern Mississippi, USA for their help with the DSC and GPC measurements, respectively.

References

- [1] Fendler JH. Membrane mimetic chemistry. New York: Wiley; 1983.
- [2] Hoffman H. Ber Bunsen-Ges Phys Chem 1994;98:1433–55.
- [3] Laughlin RG. The aqueous phase behavior of surfactants. London: Academic Press; 1994.
- [4] (a) Hoffmann H, Kalus J, Thrun H. Colloid Polym Sci 1983;261:1043–9. (b) Hargreaves WR, Deamer DW. Biochemistry 1978;17:3759–68.
- [5] (a) Menger FM, Yamasaki Y. J Am Chem Soc 1993;115:3840–1. (b) Kunitake T. Angew Chem Int Ed Engl 1992;31:709–26. (c) Fuhrhop JH, Demoulin C, Rosenberg J, Boettcher C. J Am Chem Soc 1990;112:2827–9. (d) Fuhrhop JH, Schnieder P, Rosenberg J, Boekema E. J Am Chem Soc 1989;109:3387–90. (e) Tachibana T, Yoshizumi T, Hori K. Bull Chem Soc Jpn 1979;52:34–41.
- [6] (a) Mohanty A, Dey J. Langmuir 2004;20:8452–9. (b) Dey J, Roy S. Langmuir 2003;19:9625–9.
- [7] (a) Zhang YJ, Jin M, Lu R, Song Y, Jiang L, Zhao Y. J Phys Chem B 2002;106:1960–7. (b) Boettcher C, Schade B, Fuhrhop JH. Langmuir 2001;17:873–7. (c) Borocci S, Mancini G, Cerichelli G, Luchetti L. Langmuir 1999;15:2627–30. (d) Imae T, Takahashi Y, Muramatsu H. J Am Chem Soc 1992;114:3414–9. (e) Vollhardt D, Gehlert U. J Phys Chem B 2002;106:4419–23. (f) Kawasaki H, Souda M, Tanaka S, Nemoto N, Karlsson G, Almgren M, et al. J Phys Chem B 2002;106:1524–7.
- [8] (a) Lasic DD, Barenholz Y, editors. Handbook of nonmedical applications of liposomes, vol. 4. New York: CRC Press; 1996. (b) Lasic DD. In: Rosoff M, editor. Vesicles, vol. 62. New York: Marcel Dekker; 1996. p. 447–76. (c) Lasic DD. Liposomes in gene delivery. New York: CRC Press; 1997. (d) Meager A, editor. Gene therapy technologies, applications, and regulations. New York: Wiley; 1999. (e) Lasic DD, Needham D. Chem Rev 1995;95:2601–28. (f) Sumida Y, Masuyama A, Takasu M, Kida T, Nakatsuji Y, Ikeda I, et al. Langmuir 2001;17:609–12. (g) Fendler JH, Tundo P. Acc Chem Res 1984;17:3–8.
- [9] (a) Lundhal P, Yang Q. J Chromatogr 1991;544:283–304. (b) Hong M, Weekley BS, Grieb SJ, Foley JP. Anal Chem 1998;70:1394–403 [and the references there in]. (c) Mohanty A, Dey J. J Chem Soc Chem Commun 2003;1384–5.
- [10] (a) Fendler JH. Acc Chem Res 1980;13:7–13. (b) Madani H, Kaler EW. Langmuir 1990;6:125–32.
- [11] Larrabee CE, Sprague ED. J Polym Sci Polym Lett Ed 1979;17:749–51.
- [12] (a) Kunitake T, Nakashima N, Takarabe K, Tsuge A, Yanagi H. J Am Chem Soc 1981;103:5945–7. (b) Tundo P, Kippenberger DJ, Klahn PL, Pietro NE, Jao TC, Fendler JH. J Am Chem Soc 1982;104:456–61. (c) Regen SL, Czech B, Singh A. J Am Chem Soc 1980;102:6638–40.
- [13] Mueller A, O'Brien DF. Chem Rev 2002;102:727–57.
- [14] Bader H, Ringsdorf H, Skura J. Angew Chem Int Ed Engl 1981;20:91–2.
- [15] (a) Emmanouil V, Ghoul MEI, Andre-barres C, Guidette B, Rico-Lattes I, Lattes A. Langmuir 1998;14:5389–95. (b) Fuhrhop JH, Blumtritt P, Lehmann C, Luger P. J Am Chem Soc 1991;113:7437–9. (c) Frankel DA, O'Brien DF. J Am Chem Soc 1991;113:7436–7. (d) Köning J, Boettcher C, Winkler H, Zeidler E, Talmon Y, Fuhrhop JH. J Am Chem Soc 1993;115:693–700. (e) Shinitzky M, Haimovitz R. J Am Chem Soc 1993;115:12545–9.

- (f) Song J, Cheng Q, Kopta S, Stevens R. *J Am Chem Soc* 2001;123:3205–13.
- (g) Bhattacharyya S, Krishnan-Ghosh Y. *Chem Commun* 2001;185–6.
- (h) Luo X, Liu B, Liang Y. *Chem Commun* 2001;1556–7.
- [16] (a) Du X, Hlady V. *J Phys Chem B* 2002;106:7295–9.
- (b) Du X, Liang Y. *J Phys Chem B* 2001;105:6092–6.
- (c) Du X, Liang Y. *J Phys Chem B* 2000;104:10047–52.
- (d) Miyagishi S, Takeuchi N, Asakawa T, Inoh M. *Colloid Surf A: Physicochem Eng Aspects* 2002;197:125–32.
- (e) Bella J, Borocci S, Mancini G. *Langmuir* 1999;15:8025–31.
- (f) Hoffmann F, Huhnerfuss H, Stine K. *Langmuir* 1998;14:4525–34.
- (g) Parazak DP, Uang JYJ, Turner B, Stine K. *Langmuir* 1994;10:3787–93.
- [17] (a) Takahara M, Moriyuki H, Yoshimura I, Yoshida R. *J Am Oil Chem Soc* 1972;49:143.
- (b) Takehara M. *Colloids Surf* 1989;38:149–67.
- [18] Roy S, Dey J. *Langmuir* 2005;21:10362–10369.
- [19] (a) Clothier J, Tomellini S. *J Chromatogr A* 1996;723:179–87.
- (b) Desbene P, Fulchic C. *J Chromatogr A* 1996;749:257–69.
- (c) Mechref Y, Elrassi Z. *Chirality* 1996;8:518–24.
- (d) Hara S. and Dobashi A. *Japan Patent* 92; 1992 149, 205.
- (e) Hara S. and Dobashi A. *Japan Patent* # 92; 1992 149, 206.
- (f) Chu DY, Thomas JK. *Macromolecules* 1991;24:2212–6.
- (g) Yrabe HH, Shamsi SA, Warner IM. *Anal Chem* 1999;71:3992–9.
- (h) Palmer CP. *Electrophoresis* 2000;21:4054–72 [and references therein].
- [20] (a) Palmer CP, Terabe SJ. *Microcolumn Sep* 1996;8:115–21.
- (b) Palmer CP, Terabe S. *Anal Chem* 1997;69:1852–60.
- (c) Shamsi SA, Akbay C, Warner IM. *Anal Chem* 1998;70:3078–83.
- (d) Akbay C, Warner IM, Shamsi SA. *Electrophoresis* 1999;20:145–51.
- (e) Haynes III JL, Yrabe HH, Warner IM, Shamsi SA. *Electrophoresis* 2000;21:1597–605.
- [21] Lapidot Y, Rappoport S, Wolman YJ. *Lipid Res* 1967;8:142–5.
- [22] Yeoh KW, Chew CH, Gan LM, Koh LL, Teo HH. *J Macromol Sci Chem A* 1989;26:663–80.
- [23] Fujimoto C, Fujise Y, Kawaguchi S. *J Chromatogr A* 2000;871:415–25.
- [24] Okabe S, Sugihara S, Aoshima S, Shibayama M. *Macromolecules* 2003;36:4099–106.
- [25] (a) Kalyansundaram K. *Photophysics of microheterogeneous systems*. New York: Academic Press; 1988.
- (b) Thomas JK. *The chemistry of excitation at interfaces: ACS monograph*. vol. 181. Washington, DC: American Chemical; 1984.
- (c) Winnik FM, Regismond STA. *Colloid Surf A* 1996;118:1–39.
- [26] Dong DC, Winnik MA. *Photochem Photobiol* 1982;35:17–21.
- [27] Winnik FM, Regismond STA. *Colloid Surf A* 1996;118:1–39.
- [28] Shinitzky M, Barenholz Y. *J Biol Chem* 1974;249:2652–7.
- [29] (a) Cogan U, Schinitzky M, Weber G, Nishida T. *Biochemistry* 1973;12:521–8.
- (b) Zachariasse KA, Kuhnle W, Weller A. *Chem Phys Lett* 1980;73:6–11.